Vibrational spectroscopy and crystal structure analysis of two polymorphs of the di-amino acid peptide cyclo(L-Glu-L-Glu)

ARTICLE *in* JOURNAL OF RAMAN SPECTROSCOPY · JANUARY 2009

Impact Factor: 2.67 · DOI: 10.1002/jrs.2467

7 AUTHORS, INCLUDING:

Andrew P. Mendham
University of Greenwich
23 PUBLICATIONS **180** CITATIONS
SEE PROFILE

Rex A. Palmer
University of London
189 PUBLICATIONS **2,130** CITATIONS
SEE PROFILE

Martin John Snowden
University of Greenwich
123 PUBLICATIONS **3,091** CITATIONS
SEE PROFILE

Babur Chowdhry
University of Greenwich
218 PUBLICATIONS **4,192** CITATIONS
SEE PROFILE

Research Article

Journal of RAMAN SPECTROSCOPY

Received: 5 May 2009 Accepted: 2 August 2009 Published online in Wiley Interscience: 6 October 2009

(www.interscience.wiley.com) DOI 10.1002/jrs.2467

Vibrational spectroscopy and crystal structure analysis of two polymorphs of the di-amino acid peptide cyclo(L-Glu-L-Glu)

Andrew P. Mendham,[a] Rex A. Palmer,[b]* Brian S. Potter,[b] Trevor J. Dines,[c] Martin J. Snowden,[a] Robert Withnall[d] and Babur Z. Chowdhry[a]*

Cyclo(L-Glu-L-Glu) has been crystallised in two different polymorphic forms. Both polymorphs are monoclinic, but form 1 is in space group $P2_1$ and form 2 is in space group $C2$. Raman scattering and FT-IR spectroscopic studies have been conducted for the *N,O*-protonated and deuterated derivatives. Raman spectra of orientated single crystals, solid-state and aqueous solution samples have also been recorded. The different hydrogen-bonding patterns for the two polymorphs have the greatest effect on vibrational modes with N–H and C=O stretching character. DFT (B3-LYP/cc-pVDZ) calculations of the isolated cyclo(L-Glu-L-Glu) molecule predict that the minimum energy structure, assuming C_2 symmetry, has a boat conformation for the diketopiperazine ring with the two L-Glu side chains being folded above the ring. The calculated geometry is in good agreement with the X-ray crystallographic structures for both polymorphs. Normal coordinate analysis has facilitated the band assignments for the experimental vibrational spectra.

Supporting information may be found in the online version of this article.

Keywords: cyclic di-amino acid peptides; X-ray crystallography; *ab initio* calculations; vibrational spectra

Introduction

Cyclic di-amino acid peptides (CDAPs) possess a six-membered ring, and both amide bonds adopt the *cis* conformation.[1] Previous work has shown that CDAPs can exist as different crystalline polymorphs. For example, X-ray structures of two crystalline polymorphs of cyclo(D-Ala-L-Ala) have been reported,[2,3] where both crystalline forms are monoclinic. The diketopiperazine (DKP) ring systems of both polymorphs are slightly distorted from planarity, but the main difference is the hydrogen bonding involved in both the crystal lattices. In one form, the molecules are linked together in ribbons but in the other form the molecules are hydrogen bonded in layers.[2,3] A detailed Raman and IR study has also been carried out on both the crystallographic forms of cyclo(D-Ala-L-Ala).[4] Spectroscopic differences, particularly with respect to vibrational modes involved in hydrogen bonding, were noted with respect to the two polymorphs investigated. A number of other X-ray structures have been reported for symmetrically substituted CDAPs. For example, both cyclo(Gly-Gly)[5] and cyclo(L-Ser-L-Ser)[6] have a near-planar ring conformation, whereas cyclo(L-Met-L-Met),[7,8] cyclo(L-Asp-L-Asp),[9] and cyclo(L-Ala-L-Ala)[2] have ring geometries adopting a boat conformation in the solid state. Other spectroscopic techniques such as nuclear magnetic resonance (NMR)[10,11] and circular dichroism (CD)[1] have been used to determine the structure and conformation of DKPs in the solution state, and microwave spectroscopy has been used to investigate the boat conformation found for the DKP ring of cyclo(Gly-Gly) in the gaseous state.[12] Vibrational spectroscopic studies have been carried out on cyclo(Gly-Gly)[13] and the crystalline polymorphs of cyclo(D-Ala-L-Ala),[4] which has included single-crystal Raman spectroscopy and examination of isotopically substituted derivatives of both molecules. Indeed quantum-chemical calculations have also played a part in structural analysis.[14] As part of our ongoing research into the structure and conformation of the *cis* amide group, we have reported on the vibrational spectroscopic and theoretical calculations on a number of different of CDAPs, such as cyclo (L-Ala-Gly),[15] cyclo (L-Ala-L-Ala),[15] cyclo(L-Met-L-Met),[8] cyclo(L-Ser-L-Ser),[15] and cyclo(L-Asp-L-Asp).[15] It is apparent from these studies that the location of certain vibrational modes, particularly those associated with N–H character, are highly dependent on the strength of hydrogen bonding in the crystal lattice. This has also been proved to be true when examining the crystalline polymorphs of cyclo(D-Ala-L-Ala).[4]

In the current study, we report a structural analysis of cyclo(L-Glu-L-Glu), which we have shown to exist in two polymorphic forms. The corresponding linear di-amino acid peptide (L-Glu-L-Glu) has only

* *Correspondence to: Rex A. Palmer, School of Crystallography, Birkbeck College, University of London, Malet Street, London WC1E 7HX, UK.*
E-mail: rex.palmer@btinternet.com

Babur Z. Chowdhry, School of Science, University of Greenwich at Medway, Central Avenue, Chatham Maritime, Kent ME4 4TB, UK.
E-mail: b.z.chowdhry@gre.ac.uk

a *School of Science, University of Greenwich at Medway, Kent ME4 4TB, UK*

b *School of Crystallography, Birkbeck College, University of London, London WC1E 7HX, UK*

c *Division of Electronic Engineering & Physics, University of Dundee, Dundee DD1 4HN, UK*

d *Wolfson Centre for Materials Processing, Brunel University, Uxbridge, Middlesex UB8 3PH, UK*

one amide linkage, which adopts the *trans* conformation and the amino acid end groups are zwitterionic. Raman and IR studies[16] have already been carried out on linear (L-Glu-L-Glu) in the solid state, with results highlighting the zwitterionic and *trans* amide character of this molecule. In this work, we have determined the crystal structures of two polymorphs of cyclo(L-Glu-L-Glu) by X-ray crystallography and have measured the IR (polymorph 1) and Raman spectra (polymorphs 1 and 2). Vibrational band assignments were facilitated by density functional theory (DFT) calculations of isolated molecules. Specifically, the changes in vibrational spectroscopic profiles for the two polymorphic forms of cyclo(L-Glu-L-Glu), with different hydrogen-bonding motifs and strengths, are highlighted. The *cis* amide II mode is not sensitive to differing hydrogen bonding strengths found in the crystal lattice of CDAPs, but shifts in band location are predicted to result from changes in conformation of the DKP ring.

Experimental

Materials

Cyclo(L-Glu-L-Glu) was obtained from Bachem Ltd (Saffron Walden, Essex, UK) and used without further purification. The purity of the CDAP was checked using ^{1}H-NMR spectroscopy and mass spectrometry and found to be >98%. Spectroscopic-grade deuterium oxide (99.98 atom%) was obtained from Sigma-Aldrich Ltd (Poole, Dorset, UK). The *N,O*-deuterated isotopomer was prepared from solution in D_2O and the powdered isotopomer was recovered using an Edwards freeze-drying apparatus.

X-ray crystallography

Cyclo(L-Glu-L-Glu) was crystallised in two polymorphic forms cyclo(L-Glu-L-Glu) polymorph 1 (form 1) and cyclo(L-Glu-L-Glu) polymorph 2 (form 2). The two different polymorphs were crystallised from aqueous solution by freezing to $-20\,^{\circ}$C for several hours followed by controlled evaporation at $+4\,^{\circ}$C for various time spans (1–20 days). As both polymorphs were found together in the crystallisation dishes, it has not been possible to specify unique crystallisation conditions for either polymorph. In general, although morphologically distinguishable, the initial crystals were too small for X-ray diffraction and were used as seeds to produce larger specimens. Both structures were determined at room temperature using Cu Kα diffraction intensity data collected on an Enraf Nonius CAD-4 automated four-circle diffractometer equipped with a graphite monochromator. CAD-4 Express Software[17] was used for cell parameter determination and refinement as well as data reduction. Accurate cell parameters were determined for each crystal from 25 reflections ($25^{\circ} < \omega < 28^{\circ}$). For data collection, $\omega - 2\theta$ scans were used under computer control. Intensities of 2223 reflections were measured for cyclo(L-Glu-L-Glu) polymorph 1, and 1753 reflections for cyclo(L-Glu-L-Glu) polymorph 2, both for $\theta < 74^{\circ}$. Neither crystal showed any significant variations in the intensities of the three standard reflections during the course of data collection. Lorenz and polarisation corrections were applied, but corrections for absorption effects were not applied. Both crystal structures were solved by Direct Methods in the program SHELXS-86[18] and refined using SHELXL-97,[19] both implemented in the WinGX system of programs.[20] Non-hydrogen atoms were refined anisotropically by full-matrix least squares methods. Hydrogen atom positions were added geometrically using the program. NH hydrogen positions were then refined freely, and other H atoms were refined in riding mode. All H atoms were refined with anisotropic temperature factors. Geometrical calculations were made with the programs PARST and PLATON[21] as implemented in WinGX. The programs ORTEP[22] and POVRAY,[23] also as implemented in WinGX, were used to prepare Fig. 2(a) and (b).

For cyclo(L-Glu-L-Glu) polymorph 1, in the final refinement cycles there were 1991 data to 177 parameters, resulting in a final goodness-of-fit on F^2 of 1.087 and final R indices [$I > 2\mathrm{sigma}(I)$] of $R1 = 0.0437$, $wR2 = 0.1058$. The largest and smallest difference electron density regions were 0.179 and -0.187 e Å^{-3}, respectively. The absolute structure parameter[24] is $-0.2(4)$, which confirms with certainty that the correct absolute configuration has been assigned.

For cyclo(L-Glu-L-Glu) polymorph 2, in the final refinement cycles there were 1091 data to 89 parameters, resulting in a final goodness-of-fit on F^2 of 1.060 and final R indices [$I > 2\mathrm{sigma}(I)$] of $R1 = 0.0347$, $wR2 = 0.0920$. The largest and smallest difference electron density regions were 0.168 and -0.154 e Å^{-3}, respectively. The absolute structure parameter[24] is 0.0(3), which confirms with certainty that the correct absolute configuration has been assigned. All figures show both molecules in their correct absolute configuration. The data for these crystal structures were deposited at the Cambridge Crystallographic Data Centre (CCDC) and assigned the following identification codes: polymorph 1, CCDC 252646, polymorph 2, CCDC 261395.

Measurement of vibrational spectra

Raman spectra of cyclo(L-Glu-L-Glu) containing naturally abundant isotopes and its *N,O*-deuterated isotopomer were examined using a LabRam Raman spectrometer (Horiba Jobin Yvon). The spectrometer is equipped with a 1800 grooves/mm holographic grating, a holographic notch filter, a Peltier-cooled CCD (MPP1 chip) for detection, and an Olympus BX40 microscope. A He–Ne laser provided exciting radiation of wavelength of 632.8 nm and a power of 8 mW at the sample. Raman spectra of solid-state samples were collected at room temperature on a microscope slide using a microscope objective of 10× magnification to focus the laser beam. A backscattering (180° between excitation and collection) geometry was used in all experiments. Solution-phase (H_2O or D_2O) spectra were acquired using a 1-cm path length quartz cuvette. The concentration of aqueous cyclo(L-Glu-L-Glu) used was 40 mg/ml. The temperatures of the solution samples of the CDAPs were raised in order to increase their solubility, thereby improving the signal-to-noise ratios of the spectra. The quartz cuvette was mounted in a temperature-controlled cell holder maintained at $\sim 70\,^{\circ}$C. A macro lens of 40 mm focal length was used to focus the laser beam and collect the back scattered light in these experiments.

For the solution Raman spectra, each spectral scan was collected for 20 s using 15 accumulations. In addition to the Raman solid-state (powder) spectra, single crystals of polymorphs 1 and 2 were mounted on a glass fibre and attached to an arc goniometer head. Raman spectra of the crystal faces were recorded using a 50× long-working-distance objective, and polarisation analysers were used as necessary. For solid-state samples and single-crystal experiments, each spectral scan was collected for 20 s using 15 accumulations. The Raman instrument was calibrated using the ν_1 line of silicon at 520.7 cm^{-1}. Centring of the silicon line was checked by using the frequencies of the principal lines of a neon lamp.

IR spectra (40 scans) were recorded on a Perkin Elmer Paragon 1000 FT-IR instrument operating at a resolution of 1 cm^{-1} in the 450–4000 cm^{-1} range. A dry nitrogen gas purge was maintained in the sample compartment to facilitate a simpler background subtraction. Solid-state samples were examined as pressed KBr discs. Unfortunately, due the limited quantity of polymorph 2, it was not possible to collect a suitable infrared solid-state spectrum.

Computational studies

DFT calculations for cyclo(L-Glu-L-Glu) were performed using the Gaussian 98 program,[25] with the hybrid SCF-DFT method B3-LYP, which incorporates Becke's three-parameter hybrid functional[26] and the Lee, Yang, and Parr correlation functional.[27] All calculations were performed using the cc-pVDZ basis set.[28] Geometry optimisation was carried out by assuming the molecule to have C_2 symmetry. The vibrational spectra were calculated at the optimised geometry. For computation of the potential energy distributions (PEDs) associated with the vibrational modes, the Cartesian force constants obtained from the Gaussian 98 output were converted to force constants expressed in terms of internal coordinates. Scaling factors were applied to the force constants before being input to a normal coordinate analysis program derived from those of Schachtsneider.[29] A full set of internal coordinates, including all bond angles and torsional angles, was reduced to a set of $3N - 6$ symmetry-adapted internal coordinates, by construction of local symmetry coordinates where appropriate, e.g. for the methylene groups as well as for the in-plane and out-of-plane deformations of the six-membered DKP ring. Scaling is necessary to match the calculated harmonic vibrations with the observed vibrations, which are anharmonic. Scaling of force constants, expressed in internal coordinates, was applied according to the following formula:

$$f_{ij}^{\text{scaled}} = f_{ij}^{\text{calc}} \sqrt{s_i s_j}$$

where s_i and s_j are scale factors relating to internal coordinates i and j, following the Pulay SQM-FF method.[30] We have sought to avoid the use of a large number of adjustable parameters and have chosen the scale factors below to give the best fit to the experimental data. In order to enable meaningful comparisons, these scaling factors were chosen to be identical to those used in B3-LYP/cc-pVDZ calculations on other CDAPs.[8,15]

N–H stretch	0.80
C–H stretch	0.91
N–H, C–H deformation	0.92
C═O stretch	0.86
All others	0.98

The very low scaling factors for N–H and C═O stretches are a consequence of intermolecular hydrogen bonding (and hence longer bond distances) in the solid state and aqueous solution, whereas the calculations were performed on the assumption of isolated gas-phase molecules.

IR and Raman intensities were computed from the Cartesian dipole and polarisability derivatives of the Gaussian 98 output, which were transformed to internal coordinates and subsequently to normal coordinates. Scaling of force constants causes some re-distribution of internal coordinates within the normal coordinates and therefore also some small changes in IR and Raman intensities with respect to those listed in the Gaussian 98 output.

Results and Discussion

X-ray structures of the two polymorphs of cyclo(L-Glu-L-Glu)

Both polymorphic forms of cyclo(L-Glu-L-Glu) are monoclinic (Table 1) with form 1 occupying space group $P2_1$ and form 2 occupying space group $C2$, both with two molecules per unit cell. This means that in form 2 the molecules have the required exact (crystallographic) symmetry 2 or C_2. In form 1, there is no required symmetry, but the molecular geometry with respect to bond lengths, bond angles, and torsion angles (conformation) is very close to that of form 2. Because of the required symmetry in form 2, only half of the atoms are input to the crystallographic calculations, the other half being generated by application of 2-fold symmetry and corresponding pairs of atoms. Figure 1 shows a sketch of the molecule with complete atom numbering for polymorph 1. The crystal structures are different (Fig. 2(b) and (c)) by virtue of different hydrogen-bonding schemes (Fig. 3). In form 1, there are H-bonded layers involving four hydrogen bonds, whereas in form 2 only one unique H-bond is involved plus the 2-fold generated ones. In both structures, the parallel H-bonded layers are packed at van der Waals distances. In both polymorphs, all non-H atoms excluding the carboxylate oxygens O24 and O25, O30 and O31, lie, within 0.2Å, in one plane, as illustrated in Fig. 2(b) and (c).

If we first consider the bond lengths (Table S1, Supporting Information), the most significant differences between polymorph 1 and 2 occur for the LHS chain at O25–C23 with values of 1.323(2) and 1.302(2) Å, and O24–C23 with values of 1.217(3) and 1.228(2) Å, respectively. In the case of the torsional angles, while the general trends in conformational features are parallel, most torsion angles differ by more than 3σ, and are therefore significant. This indicates, as might be expected, that there is some flexibility in both the side chain and ring features of the structure. In both polymorphs, the DKP rings are in the boat conformations. Ignoring atom type differences, the rings display approximate *mm*2 symmetry. If atom types are considered, this, of course, reduces to approximate symmetry 2(C_2) in polymorph 1 and exact symmetry 2(C_2) in polymorph 2 (the asymmetry parameters for the two polymorphs are tabulated in Table S2(a), Supporting Information).

Calculated/experimental structures and vibrational spectra

The atom numbering scheme for cyclo(L-Glu-L-Glu) is shown in Fig. 1. The computed molecular structure for cyclo(L-Glu-L-Glu) is compared with the X-ray structures for the two different crystalline polymorphs in Fig. 2. Calculated bond lengths, bond angles, and selected torsion angles are compared with the experimental data in Table S1 (Supporting Information). Full geometry optimisation, assuming C_2 symmetry, predicts a boat conformation for the DKP ring with the two L-Glu side chains being folded above the ring. It is important to note that the calculated structure (Fig. 2(a)) is based on a single molecule in the gas phase and does not take into account intermolecular forces such as hydrogen bonding. The X-ray crystallographic structures of form 1 and form 2 of cyclo(L-Glu-L-Glu) reported herein show that the DKP ring displays a boat conformation, for both polymorphs, with the two L-Glu side chains being folded above the ring, although it is clear that for form 1, the two side chains are not superimposable after a C_2 symmetry operation, but form 2 shows exact C_2 symmetry.

The bond lengths, (Table S1, Supporting Information) generally show a good correlation between calculated and experimental data, although large differences are observed with respect to the N–H and O–H bond lengths. Our calculations predict an N–H

Journal of RAMAN SPECTROSCOPY

Table 1. Crystal data and structure refinement for cyclo(L-Glu-L-Glu), polymorphs 1 and 2

Identification code	Cyclo(L-Glu-L-Glu) form 1	Cyclo(L-Glu-L-Glu) form 2
Empirical formula	$C_{10}H_{14}N_2O_6$	$C_{10}H_{14}N_2O_6$
Formula weight	258.23	258.23
Temperature (K)	293(2)	293(2)
Wavelength (Å)	1.54180	1.54180
Crystal system	Monoclinic	Monoclinic
Space group	$P2_1$	$C2$
Unit cell dimensions (Å)	$a = 6.7441(4)$	13.9539(10)
	$b = 10.8592(11)$	6.6639(10)
	$c = 7.8397(5)$	6.1479(10)
α (°)	90.000(6)	90.0000(10)
β (°)	94.498(5)	100.080(10)
γ (°)	90.000(7)	90.0000(10)
Volume (Å^3) 572.38(8) Å^3	572.38(8)	562.85(13)
Z	2	2 (required molecular symmetry 2 (C_2))
Density (calc.; mg/m^3)	1.498	1.524
Absorption coefficient (mm^{-1})	1.076	1.094
F(000)	272	272
Crystal size (mm^3)	0.50 × 0.35 × 0.30	0.40 × 0.35 × 0.10
Theta range for data collection (°)	5.66 to 74.24	7.32 to 74.17
Index ranges	$-8 \le h \le 8, -13 \le k \le 13, 0 \le l \le 9$	$-17 \le h \le 17, -8 \le k \le 8, -6 \le l \le 7$
Reflections collected	2223	1753
Independent reflections	1991 (R(int) = 0.0209)	1091 (R(int) = 0.0192)
Completeness to theta (%)	74.24° (93.7)	74.17° (95.1)
Refinement method	Full-matrix least-squares on F^2	Full-matrix least-squares on F^2
Data/restraints/parameters	1991/1/177	1091/1/89
Goodness-of-fit on F^2	1.087	1.060
Final R indices ($I > 2$sigma(I))	$R1 = 0.0437$, $wR2 = 0.1058$	$R1 = 0.0347$, $wR2 = 0.0920$
R indices (all data)	$R1 = 0.0560$, $wR2 = 0.1111$	$R1 = 0.0384$, $wR2 = 0.0939$
Absolute structure parameter	−0.2(4)	0.0(3)
Extinction coefficient	0.0127(10)	0.0050(6)
Largest diff. peak and hole (e.Å^{-3})	0.179 and −0.187	0.168 and −0.154

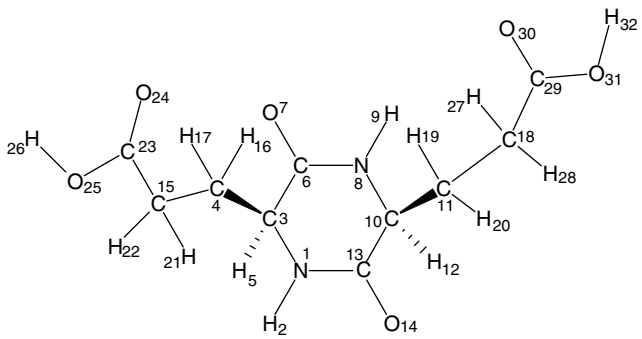

Figure 1. Schematic showing the chemical structure and atom numbering scheme for cyclo(L-Glu-L-Glu).

bond length of 1.02 Å and an O–H bond length of 0.98 Å. The X-ray data, for both polymorphic forms, shows that the N–H and O–H bond lengths are 0.86(2) and 0.82 Å, respectively. However, only the N–H bond lengths were refined, as the O–H hydrogens were geometrically fixed in the least-squares program (HFIX). This discrepancy is a consequence of the poor ability of X-ray diffraction to accurately locate the positions of hydrogen atoms. We expect the actual N–H and O–H bond distances to be slightly longer than the calculated values due to intermolecular hydrogen bonding. Smaller differences between computed and experimental values are observed for the C–N (amide) and C–O (carboxylic acid) bond lengths, where differences of between ~0.03 and 0.05 Å are observed. This is undoubtedly due to the effect of intermolecular hydrogen bonding.

A comparison between the calculated and experimental bond angles (Table S1, Supporting Information) show that there is a good correlation between the two sets of data. Only small differences are observed for the bond angles between C13–N1–H2, C13–N1–C3, and C23–O25–H26. Our calculated results predict the following bond angles: 114.0°, 127.1°, and 106.0°, respectively. The experimental bond angles for cyclo(L-Glu-L-Glu) are 113.32°, 126.0(2)°, and 109.5° (form 1) and 117.5(2)°, 124.9(1)°, and 109.5° (form 2), respectively. Hydrogen-bonding effects may account for the above differences.

Some of the torsion angles, illustrated in Table S1 (Supporting Information), can give valuable information as to the extent of the puckering of the DKP ring and the geometry of the amide bond. For example, the values of the torsional angles ω, ϕ, and ψ ($C_i - N_{i+1}$, $N_i - C^{\alpha}{}_i$, and $C^{\alpha}{}_i - C'_i$, respectively) are all important in relation to the geometry of the endocyclic amide bonds. Calculated torsional angles of cyclo(L-Glu-L-Glu) for ω, ϕ, and ψ are −6.5°, 25.3°, and −18.1°, respectively, whereas the experimental data shows ω, ϕ, and ψ values of 11.2° and 4.2°, −37.6° and −30.6°, and 22.1° and 28.8° (polymorph 1, with C_1 symmetry), respectively. For

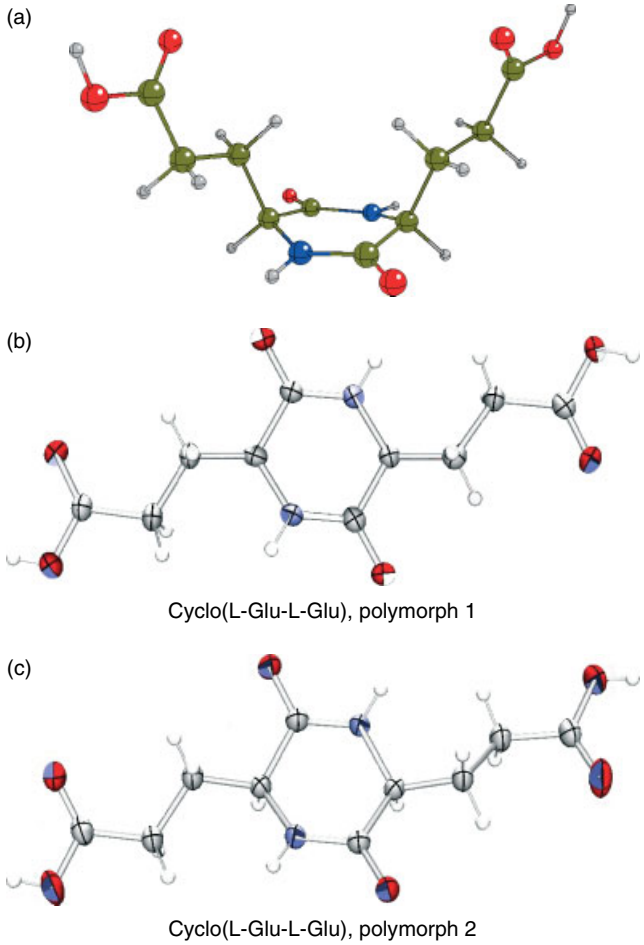

Figure 2. (a) Calculated least energy boat conformation of cyclo(L-Glu-L-Glu); (b) and (c) experimental X-ray crystallographic structures for the two crystalline polymorphs of cyclo(L-Glu-L-Glu).

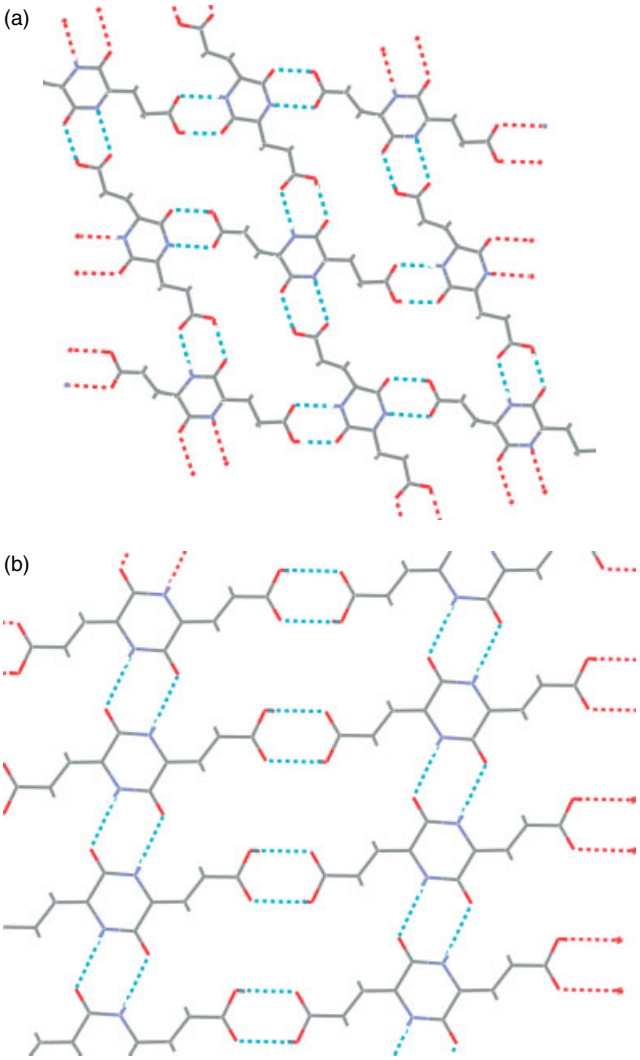

Figure 3. (a) Hydrogen-bonding in polymorph 1 of cyclo(L-Glu-L-Glu) (from X-ray crystallographic data). (b) Hydrogen-bonding in polymorph 2 of cyclo(L-Glu-L-Glu) (from X-ray crystallographic data).

polymorph 2 with C_2 symmetry, the values of ω, ϕ, and ψ are 4.3°, −38.8°, and 29.7°, respectively. These results illustrate that both experimental and calculated structures show that both *cis* amide groups are significantly non-planar. By taking the average of two pseudo torsional angles N1–C3–C10–N8 −180° (known as β_1) and C6–C3–C10–C13 −180° (known as β_2), a good measure of the folding of the DKP ring (β) can be established.[31] The calculated geometry of cyclo(L-Glu-L-Glu) shows a β value of 22.4°, whereas the experimental results indicate β values of 32.4° (form 1) and 35.5° (form 2). Both results indicate that the DKP ring deviates considerably from planarity into a boat conformation. Our results compare favourably with the boat conformation previously reported by authors who used density functional B3-LYP methods, but with a lower level of theory (6-31G(d))[14] than used in the present study.

Simulated IR and Raman spectra, calculated by convolution with a Lorentzian line shape (full width at half-maximum = 10 cm^{-1}), are shown in Figs 4 and 5. The scaled vibrational wavenumbers, together with their PEDs, are compared with the experimental data for protonated cyclo(L-Glu-L-Glu) in Table 2 and for the deuterated species in Table 3. Generally, the calculated spectra agree quite well with the experimental data. There is a good correlation between experimental (Raman and IR) spectra and calculated band positions, although large differences are observed with respect to modes involved in hydrogen bonding. This is as expected, especially as significant differences between calculated and experimental bond lengths involving N–H and O–H groups have already been highlighted.

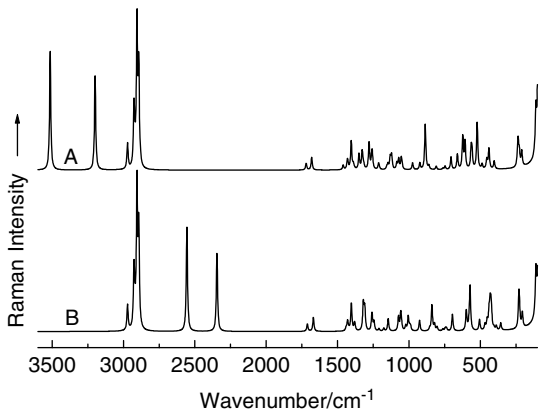

Figure 4. Calculated Raman spectra of cyclo(L-Glu-L-Glu); A = non-deuterated, B = *N,O*-deuterated.

Table 2. Experimental and calculated wavenumber (in cm^{-1}) locations of vibrational bands of cyclo(L-Glu-L-Glu) polymorphs

IR (solid) (1)	Raman (solid) (1)	Raman (solid) (2)	Calculated	% PEDs	Raman (aq.)
3288	3287	3193	3514 *A*	ν(OH) (100)	
			3514 *B*	ν(OH) (100)	
3214	3218	3117	3199 *A*	ν(NH) (100)	
			3198 *B*	ν(NH) (100)	
3085					
3063	3064	3067			
2994	2994	2996	2972 *A*	$\nu_{as}(CH_2)$[a] (99)	
2985	2984		2971 *B*	$\nu_{as}(CH_2)$ (89)	
	2972	2977	2927 *A*	$\nu_s(CH_2)$ (13), $\nu_{as}(CH_2')$ (85)	
			2927 *B*	$\nu_{as}(CH_2')$[b] (89)	
2947	2945	2942	2920 *A*	ν(CH) (13), $\nu_s(CH_2)$ (70), $\nu_{as}(CH_2')$ (10)	2938
	2925	2923	2918 *B*	ν(CH) (17), $\nu_s(CH_2)$ (70)	
2916	2917	2894	2905 *A*	ν(CH) (85), $\nu_s(CH_2)$ (11)	
2873	2874	2866	2905 *B*	ν(CH) (82), $\nu_s(CH_2)$ (14)	
2849	2847		2893 *A*	$\nu_s(CH_2')$ (99)	
			2893 *B*	$\nu_s(CH_2')$ (99)	
2755	2742	2757			
2738		2720			
2689	2684	2680			
2678					
2607	2626	2629			
2576	2581	2584			
2542	2566				
2506					
2472					
2149					
2105					
1899					
1858	1778				
1708			1719 *B*	ν(C20O24) (81)	
	1697	1708	1721 *A*	ν(C20O24) (81)	1714
	1653	1667	1681 *A*	ν(C6O7) (71), ν(C6N8) (10)	1668
1635			1681 *B*	ν(C6O7) (71), ν(C6N8) (11)	
	1612	1648			
	1493	1491	1461 *A*	ν(C3C6)(12), ν(C6N8)(31), δ_{ip}(NH)(17), ω(CCH) (10)	1507
1463					
	1451	1463	1429 *A*	$\delta(CH_2)$ (89)	
1447	1447	1443	1432 *B*	ν(C6N8) (14), $\delta(CH_2)$ (56)	1436
1432			1426 *B*	ν(C6N8) (25), $\delta(CH_2)$ (34)	
1424	1422	1419	1404 *A*	$\delta(CH_2')$ (93)	1422
1409	1408		1404 *B*	$\delta(CH_2')$ (95)	
	1379	1375	1390 *A*	ν(C-O) (13), ν(C15C20) (15), $\omega(CH_2)$ (10), $\omega(CH_2')$ (33)	
1373			1387 *B*	ν(C-O) (13), ν(C15C20) (15), $\omega(CH_2')$ (30)	
1351			1381 *B*	ν(C3C6) (15), ν(C6N8) (10), δ_{ip}(NH) (53), δ_{ip}(CO) (11)	
	1344	1351	1350 *A*	ν(N1C3) (13), δ_{ip}(NH) (34), ω(CCH) (10)	
1320	1317	1318	1328 *A*	ω(CCH) (13), $\omega(CH_2)$ (44)	1310
			1322 *B*	$\omega(CH_2)$ (45)	
1294	1293	1291	1316 *B*	ν(N1C3) (14), δ(CCH) (20), ω(CCH) (23), $\tau(CH_2)$ (19)	
	1286	1284	1279 *A*	ν(C6N8) (12), δ_{ip}(NH) (13), δ(CCH) (15), $\tau(CH_2)$ (12)	1284
		1258	1262 *A*	δ(CCH) (17), $\tau(CH_2)$ (17), $\tau(CH_2')$ (23)	
1263		1240	1259 *B*	δ(COH) (21), δ(CCH) (17), ω(CCH) (10), $\omega(CH_2')$ (23)	
1222	1223	1222	1258 *A*	ω(CCH) (21), $\tau(CH_2)$ (17), $\tau(CH_2')$ (15)	
			1256 *B*	$\tau(CH_2)$ (33), $\tau(CH_2')$ (42)	
	1214	1206	1213 *A*	δ(COH) (19), δ(CCH) (15), $\omega(CH_2)$ (26), $\omega(CH_2')$ (12)	
1204			1209 *B*	δ(COH) (15), δ(CCH) (17), $\omega(CH_2)$ (23)	
1194	1192	1198	1155 *A*	$\tau(CH_2)$ (22), $\tau(CH_2')$ (33)	
	1144	1142	1132 *A*	ν(C-O) (22), δ(COH) (17)	1141

Table 2. (*Continued*)

IR (solid) (1)	Raman (solid) (1)	Raman (solid) (2)	Calculated	% PEDs	Raman (aq.)
1124	1124	1120	1147 *B*	$\tau(CH_2)$ (28), $\tau(CH_2')$ (36)	
1096	1096	1097	1121 *A*	ν(N1C3) (24), ν(C-O) (14), δ(COH) (10), δ_{ip}(NH) (11)	1095
			1129 *B*	ν(C-O) (33), δ(COH) (24), $\omega(CH_2')$ (13)	
	1085		1085 *B*	ν(N1C3) (30), ν(C3C4) (26), δ_{ip}(NH) (11)	
1060	1060	1063	1072 *A*	ν(C3C4) (16), ν(C4C15) (43)	1050
	999	1002	1054 *A*	ν(C3C4) (11), ν(C4C15) (23), ρ(CCH) (12), $\rho(CH_2)$ (16), $\rho(CH_2')$ (13)	
988			1074 *B*	ν(C4C15) (44)	
			1049 *B*	ν(C4C15) (16), ρ(CCH) (15), $\rho(CH_2)$ (23), $\rho(CH_2')$ (18)	
970		957	974 *A*	ν(C3C4) (33), $\rho(CH_2)$ (11), $\rho(CH_2')$ (12)	
955			964 *B*	ν(C3C4) (13), ν(C3C6) (11), δ_{ip}(ring-3) (33)	
	925	929	924 *B*	ν(N1C3) (10), ν(C3C4) (11), ν(C3C6) (10), ν(C15C20) (10)	920
892	893		886 *A*	ν(C-O) (10), ν(C15C20) (50)	865
858			861 *B*	ν(C-O) (10), ν(C15C20) (44)	
848	847	853	813 *B*	ν(C3C6) (12), δ_{ip}(ring-3) (17), $\rho(CH_2')$(17), $\omega(CO_2)$ (11)	843
823	823	818	809 *A*	$\rho(CH_2)$ (12), $\rho(CH_2')$ (19), $\omega(CO_2)$ (12)	818
793					
	785	790	762 *A*	$\rho(CH_2)$ (17), δ_{op}(CO) (28)	
			747 *B*	δ_{ip}(ring-3) (21), $\rho(CH_2)$ (20), δ_{op}(CO) (20)	
752			558 *B*	δ_{op}(NH) (83)	
734	737	762	564 *A*	δ_{op}(NH) (66)	
686	685	687	705 *A*	ν(C3C6) (10), δ_{op}(CO) (37)	
			706 *B*	$\rho(CH_2)$ (11), δ_{op}(CO) (57)	
	673				
658	660		661 *A*	$\rho(CH_2')$ (11), $\omega(CO_2)$ (12), τ(C20O25) (72)	649
			660 *B*	$\rho(CH_2')$ (12), $\omega(CO_2)$ (11), τ(C20O25) (71)	
	640	646	623 *A*	δ_{ip}(CO) (17), δ(OCO) (34)	
			624 *B*	ν(C-O) (11), δ(OCO) (55)	
	633	629	607 *A*	ν(C3C6) (12), δ_{ip}(CO) (28), δ(OCO) (16)	611
589	587	585	522 *A*	$\rho(CH_2')$ (19), $\omega(CO_2)$ (48), τ(C20O25) (26)	
	570				559
560			522 *B*	$\rho(CH_2')$ (19), $\omega(CO_2)$ (47), τ(C20O25) (26)	
	508		487 *A*	δ_{ip}(ring-1) (36), δ_{ip}(CO) (10), δ_{op}(NH) (16)	
	495	495	453 *A*	δ(OCO) (13), $\rho(CO_2)$ (36)	494
484	483	484	457 *B*	δ(OCO) (12), $\rho(CO_2)$ (43)	
475			450 *B*	N1C3) (12), τCCH) (10), δ(C3C4C15) (11), δ_{ip}(CO) (24)	
	453	452	440 *A*	ν(N1C3) (15), δ_{ip}(ring-2) (60)	460
	406	408	403 *A*	ρ(CCH) (24), δ_{ip}(CO) (11)	
	401		396 *B*	ρ(CCH) (18), δ_{ip}(CO) (33)	
	317				
	292	280	240 *B*	τCCH) (14), δ(C3C4C15) (15), δ(C4C15C20) (26), $\rho(CO_2)$ (14)	
	241	246	235 *B*	ν(C3C6) (10), ρ(CCH) (12), δ(C3C4C15) (16), $\rho(CO_2)$ (10)	
	204	236	226 *A*	τCCH) (11), δ(C3C4C15) (11), δ(C4C15C20) (31), $\rho(CO_2)$ (14)	
	171	187	210 *A*	ρ(CCH) (11), δ_{ip}(ring-1) (14), δ(C3C4C15) (17)	
		164			
	153	154	115 *A*	δ_{op}(ring-3) (28), τ(C3C4) (53)	
	134	134	110 *B*	δ_{op}(ring-1) (31), τ(C3C4) (52)	
	120	120	98 *A*	δ(C3C4C15) (20), δ(C4C15C20) (17), τ(C3C4) (12), τ(C4C15) (16)	
	103		97 *B*	δ(C3C4C15) (26), δ(C4C15C20) (31)	
			93 *B*	δ_{op}(ring-1) (30), τ(C4C15) (45), τ(C15C20) (18)	
			89 *A*	δ_{op}(ring-2) (47), τ(C4C15) (25)	
			48 *A*	δ_{op}(ring-2) (48), τ(C4C15) (15), τ(C15C20) (19)	
			38 *B*	δ_{op}(ring-1) (43), τ(C3C4) (15), τ(C4C15) (30)	
			24 *A*	τ(C3C4) (14), τ(C4C15) (11), τ(C15C20) (61)	
			23 *B*	τ(C3C4) (12), τ(C4C15) (13), τ(C15C20) (76)	
			17 *A*	δ_{op}(ring-3) (64), τ(C4C15) (19)	

[a] CH_2 refers to C4 and C11 (Fig. 1).
[b] CH_2' refers to C15 and C18.

Journal of RAMAN SPECTROSCOPY

Table 3. Experimental and calculated wavenumber (in cm^{-1}) locations of vibrational bands of *N*-deuterated cyclo(L-Glu-L-Glu) polymorphs

IR (solid) (1)	Raman (solid) (1)	Raman (solid) (2)	Calculated	% PEDs	Raman (aq.)
2997	2994	2994	2972 *A*	$\nu_{as}(CH_2)$ (90)	
			2971 *B*	$\nu_{as}(CH_2)$ (89)	
	2983				
2978	2975	2975			
2944	2946	2939			
2926	2923	2923	2927 *A*	$\nu_s(CH_2)$ (13), $\nu_{as}(CH_2')$ (85)	2934
			2927 *B*	$\nu_{as}(CH_2')$ (89)	
	2916		2920 *A*	ν(CH) (13), $\nu_s(CH_2)$ (70), $\nu_{as}(CH_2')$ (10)	
			2918 *B*	ν(CH) (17), $\nu_s(CH_2)$ (70)	
2871	2870	2891	2905 *A*	ν(CH) (85), $\nu_s(CH_2)$ (11)	
			2905 *B*	ν(CH) (82), $\nu_s(CH_2)$ (14)	
	2861	2860	2893 *A*	$\nu_s(CH_2')$ (99)	
			2893 *B*	$\nu_s(CH_2')$ (99)	
	2845	2810			
2767					
	2697	2701			
2686					
2605	2603				
2527					
	2457				
	2387				
2361	2355	2353			
	2343	2342	2345 *A*	ν(ND) (99)	
2250			2344 *B*	ν(ND) (99)	
2228	2206	2229	2556 *A*	ν(OD) (100)	
2080	2069	2119	2556 *B*	ν(OD) (100)	
		2066			
	1719				
1701			1711 *B*	ν(C20O24) (85)	
	1688		1712 *A*	ν(C20O24) (84)	1708
1663			1671 *B*	ν(C6O7) (75), ν(C6N8) (11)	
	1633	1638	1670 *A*	ν(C6O7) (77)	1645
	1624	1633			
1617					
	1467	1484	1440 *A*	ν(C3C6) (14), ν(C6N8) (39), ω(CCH) (12)	1487
1464	1463	1462	1431 *B*	$\delta(CH_2)$ (80)	
1443	1442	1442	1428 *A*	$\delta(CH_2)$ (90)	1443
	1427		1420 *B*	ν(C6N8) (41), ω(CCH) (10), $\delta(CH_2)$ (12)	
1417	1417	1417	1404 *B*	$\delta(CH_2')$ (96) 1420	
	1409	1373	1403 *A*	$\delta(CH_2')$ (94)	
	1354	1354	1382 *A*	ν(C-O) (10), ν(C15C20) (15), $\omega(CH_2)$ (15), $\omega(CH_2')$ (38)	
1362			1379 *B*	ν(C-O) (10), ν(C15C20) (15), $\omega(CH_2)$ (13), $\omega(CH_2')$ (37)	
	1340	1342			
1325	1322	1323	1320 *A*	ω(CCH) (25), $\omega(CH_2)$ (33)	1327
			1318 *B*	ω(CCH) (19), $\omega(CH_2)$ (36)	
	1311	1309	1310 *A*	ν(N1C3) (21), ω(CCH) (21), $\omega(CH_2)$ (10), $\tau(CH_2)$ (12)	
			1316 *B*	δ(CCH) (31), ω(CCH) (11), $\tau(CH_2)$ (18)	
1298	1296	1297	1260 *A*	$\tau(CH_2)$ (33), $\tau(CH_2')$ (38)	
1280			1258 *B*	$\tau(CH_2)$ (34), $\tau(CH_2')$ (35)	
	1273	1278	1245 *A*	ν(C-O) (13), δ(CCH) (28)	
1241		1223	1246 *B*	ν(C-O) (10), δ(CCH) (22)	
1212	1211	1209	1210 *A*	ν(N1C3) (15), ν(C3C6) (10), ω(CCH) (17), τ(CCH) (23), δ_{ip}(CO) (10)	
1195	1194	1195	1210 *B*	ν(N1C3) (25), δ_{ip}(ND) (18), δ_{ip}(CO) (16)	1202
	1175	1175	1176 *A*	ν(C-O) (18), $\omega(CH_2)$ (20), $\omega(CH_2')$ (35)	
1133		1132	1176 *B*	ν(C-O) (16), $\omega(CH_2)$ (15), $\omega(CH_2')$ (31)	
1123			1146 *A*	$\tau(CH_2)$ (28), $\tau(CH_2')$ (39)	

Table 3. Experimental and calculated wavenumber (in cm^{-1}) locations of vibrational bands of *N*-deuterated cyclo(L-Glu-L-Glu) polymorphs

IR (solid) (1)	Raman (solid) (1)	Raman (solid) (2)	Calculated	% PEDs	Raman (aq.)
1098			1144 *B*	$\tau(CH_2)$ (28), $\tau(CH_2')$ (37)	
	1090	1091	1073 *A*	ν(C4C15) (49)	
1068	1069	1069	1074 *B*	ν(C4C15) (50)	
	1059	1062	1058 *A*	ν(C3C4) (18), ν(C4C15) (14), ρ(CCH) (12), $\rho(CH_2)$ (16), $\rho(CH_2')$ (14)	1054
			1053 *B*	ν(C3C4) (19), ρ(CCH) (14), $\rho(CH_2)$ (20), $\rho(CH_2')$ (16)	
1042	1042	1042	1023 *B*	ν(C3C4) (18), δ_{ip}(ND) (14)	
	1030		1005 *A*	ν(C-O) (15), δ(COD) (24)	
992			994 *B*	ν(C-O) (26), δ(COD) (38)	
	981	980	988 *A*	ν(C-O) (14), ν(C3C4) (22), δ(COD) (18)	
965			926 *A*	ν(C3C6) (11), ν(C6N8) (10), δ_{ip}(ND) (44)	
939			953 *B*	ν(C3C6) (11), ν(C3C4) (12), δ_{ip}(ring-3) (30)	
	918	919			
898	896	898	855 *B*	ν(N1C3) (11), δ_{ip}(ND) (14), δ_{ip}(ring-3) (14), $\rho(CH_2')$ (12)	
856			839 *A*	ν(C15C20) (34), δ(COD) (18)	
852			821 *B*	ν(C15C20) (36), δ(COD) (18)	
	846	850			820
797	794	796	803 *A*	$\rho(CH_2)$ (14), $\rho(CH_2')$ (19), $\omega(CO_2)$ (12)	
776	773	774	762 *B*	δ_{ip}(ND) (21), $\rho(CH_2)$ (23)	
756	754	755	746 *A*	$\rho(CH_2)$ (17), δ_{op}(CO) (36)	
			737 *B*	δ_{ip}(ring-3) (22), δ_{op}(CO) (34)	
698			697 *B*	ν(C3C6) (14), $\rho(CH_2)$ (10), δ_{op}(CO) (43)	
680	681	674	695 *A*	ν(N1C3) (10), ν(C3C6) (11), ν(C6N8) (12), δ_{op}(CO) (30)	664
643			599 *A*	δ_{ip}(CO) (32)	
	636	638	595 *A*	$\rho(CH_2')$ (23), $\omega(CO_2)$ (38), τ(C20O25) (18)	
	614	607	595 *B*	$\rho(CH_2')$ (25), $\omega(CO_2)$ (44), τ(C20O25) (21)	600
578	578	558	580 *B*	ν(C-O) (11), δ(COD) (17), δ(OCO) (40), $\rho(CO_2)$ (12)	557
550		551	572 *A*	δ(COD) (14), δ(OCO) (37), $\rho(CO_2)$ (12)	
	543				
	486	488	505 *A*	ρ(CCH) (17), δ_{ip}(ring-1) (20), δ_{ip}(CO) (10), δ_{op}(NH) (16)	
480					
	474	477	467 *B*	δ(OCO) (17), $\rho(CO_2)$ (25), δ_{op}(ND) (17)	473
	448	449	453 *A*	δ_{ip}(ring-1) (20), δ_{ip}(ring-2) (25), δ_{op}(ND) (16)	
			450 *B*	ν(N1C3) (10), τCCH) (10), δ(C3C4C15) (10), δ_{ip}(CO) (18)	
			439 *A*	δ_{ip}(ring-2) (22), δ(OCO) (10), $\rho(CO_2)$ (25)	
	388	390	432 *A*	δ_{ip}(ring-2) (19), τ(C20O25) (33)	
			426 *B*	$\omega(CO_2)$ (14), τ(C20O25) (69)	
			422 *A*	δ_{op}(ND) (13), $\omega(CO_2)$ (10), τ(C20O25) (42)	
			405 *B*	δ_{ip}(CO) (13), $\rho(CO_2)$ (16), δ_{op}(ND) (38)	
			388 *B*	ρ(CCH) (11), δ_{ip}(CO) (20), δ_{op}(ND) (44)	
	311		357 *A*	ρ(CCH) (10), δ_{op}(ND) (45), δ_{op}(ring-2) (18)	
	277	278	236 *B*	ν(C3C4) (11), δ(C3C4C15) (28), δ(C4C15C20) (14)	
	234	235	225 *A*	τCCH) (12), δ(C3C4C15) (11), δ(C4C15C20) (31), $\rho(CO_2)$ (15)	
			229 *B*	ω(CCH) (10), τ(CCH) (18), δ(C4C15C20) (12), $\rho(CO_2)$ (20)	
	202		206 *A*	ρ(CCH) (11), δ_{ip}(ring-1) (14), δ(C3C4C15) (17)	
	186	187	114 *A*	δ_{op}(ring-3) (28), τ(C3C4) (53)	
	177		110 *B*	δ_{op}(ring-1) (32), τ(C3C4) (52)	
	159	161	96 *A*	δ(C3C4C15) (21), δ(C4C15C20) (18), τ(C3C4) (10), τ(C4C15) (14)	
	133	140	95 *B*	δ(C3C4C15) (26), δ(C4C15C20) (30)	
	127	127	91 *B*	δ_{op}(ring-1) (34), τ(C4C15) (44), τ(C15C20) (16)	
	113	112	89 *A*	δ_{op}(ring-2) (48), τ(C4C15) (26)	
	96		47 *A*	δ_{op}(ring-2) (47), τ(C4C15) (15), τ(C15C20) (19)	
			38 *B*	δ_{op}(ring-1) (43), τ(C3C4) (14), τ(C4C15) (31)	
			24 *A*	τ(C3C4) (13), τ(C4C15) (12), τ(C15C20) (62)	
			22 *B*	τ(C3C4) (12), τ(C4C15) (12), τ(C15C20) (77)	
			17 *A*	δ_{op}(ring-3) (64), τ(C4C15) (19)	

Journal of RAMAN SPECTROSCOPY

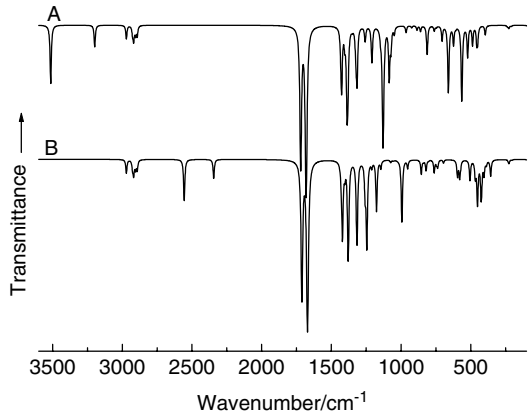

Figure 5. Calculated IR spectra of cyclo(L-Glu-L-Glu); A = non-deuterated, B = *N*,*O*-deuterated.

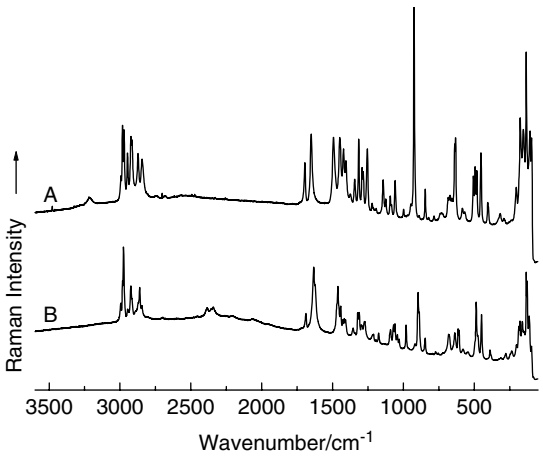

Figure 6. Raman spectra of solid state samples of cyclo(L-Glu-L-Glu) polymorph 1; A = non-deuterated and B = *N*,*O*-deuterated.

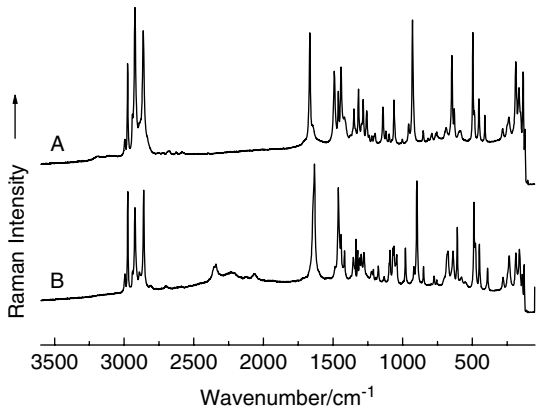

Figure 7. Raman spectra of solid state samples of cyclo(L-Glu-LGlu) polymorph 2; A = non-deuterated and B = *N*, *O*-deuterated.

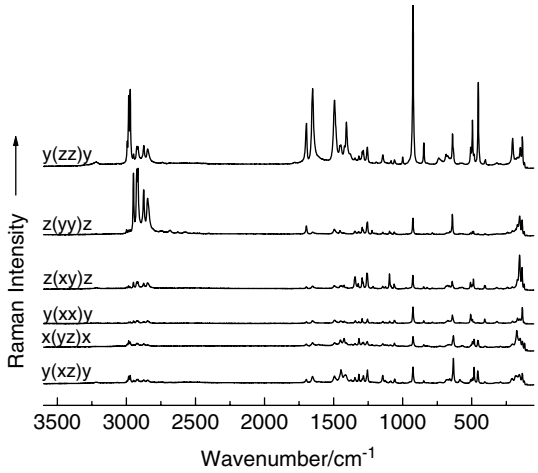

Figure 8. Single-crystal Raman spectra of cyclo(L-Glu-L-Glu) polymorph 1.

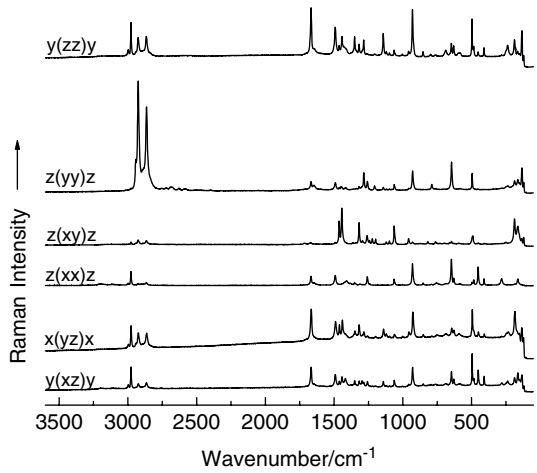

Figure 9. Single-crystal Raman spectra of cyclo(L-Glu-L-Glu) polymorph 2.

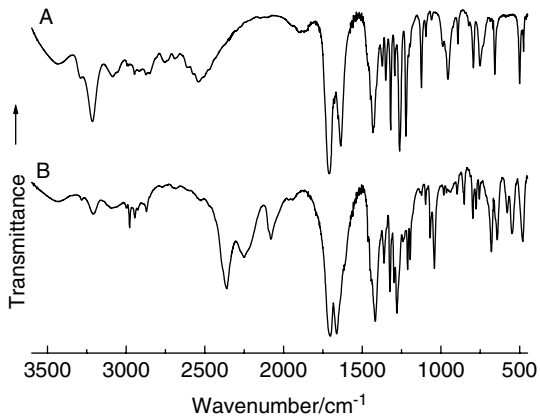

Figure 10. FT-IR spectra of solid state samples of cyclo(L-Glu-L-Glu) polymorph 1; A = non-deuterated and B = *N*,*O*-deuterated.

Vibrational assignments

Experimental Raman spectra for the two polymorphs of cyclo(L-Glu-L-Glu) in the solid state are shown in Figs 6 and 7, and single-crystal Raman spectra of the protonated polymorphs are shown in Figs 8 and 9. The IR spectrum of polymorph 1 is shown in Fig. 10 and the aqueous (H_2O and D_2O) phase Raman spectra are shown in Fig. 11. The vibrational band assignments have been made on the basis of comparison with the calculated band wavenumber positions and PEDs for cyclo(L-Glu-L-Glu). For

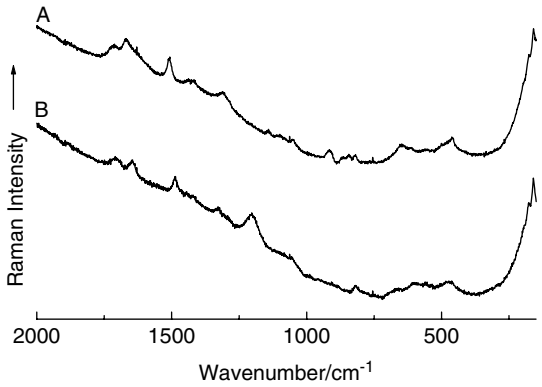

Figure 11. Aqueous solution Raman spectra of cyclo(L-Glu-L-Glu); A = non-deuterated, B = *N*,*O*-deuterated.

a molecule possessing 30 atoms, the $3N - 6$ rule suggests that cyclo(L-Glu-L-Glu) should display 84 internal vibrational bands. The calculated structure has C_2 symmetry; it is therefore predicted that there should be 43 vibrational modes with *A* symmetry and 41 vibrational modes with *B* symmetry. As expected, the Raman and IR results also show that the rule of mutual exclusion does not hold for this molecule, because it lacks a centre of symmetry. As stated previously, the crystals of both polymorphs are monoclinic, where form 1 displays space group $P2_1$ and form 2 displays space group C_2. In both forms, the factor group is isomorphic to C_2, which results in two symmetry blocks *A* and *B*. Where factor group splittings are observed, we can assign the symmetry species for each component; vibrational modes with *A* symmetry appear in the single-crystal Raman *xx*, *yy*, *zz*, and *xz* spectra and for those with *B* symmetry the bands appear in the Raman *xy* and *yz* spectra. The number of external, or lattice, modes in the crystalline polymorphs of cyclo(L-Glu-L-Glu) are different, as this is dependent on Z' (the number of molecules per primitive unit cell). In form 1, $Z' = 2$ and form 2, $Z' = 1$. Therefore, the total number of translational, rotational, and acoustic modes can be calculated by using the formula: $(3NZ') - ((3N - 6)Z')$. Thus, in form 1, we would expect 12 external modes (this includes 3 acoustic modes) and in form 2 we would expect 6 external modes (again, this includes 3 acoustic modes).

Spectral region >2000 cm^{-1}

The bands found in this region of the spectrum are due to O–H, O–D, N–H, N–D, and C–H stretching modes. It has previously been established that the two crystalline polymorphs of cyclo(D-Ala-L-Ala) have quite different N–H stretching vibrations, which are attributed to the variation in hydrogen-bonding motifs found between the two forms.[4] Indeed, in form 1, where the hydrogen bonding is described as layers, the N–H stretching vibrations in both the Raman and IR spectra are located at a higher wavenumber (~100 cm^{-1}) than that of the N–H stretching vibrations of form 2, where the hydrogen bonding is described as a chain. Additionally, the wavenumber location of the N–H stretch gives a direct relationship to the strength of the hydrogen bonding involved in the crystal lattice, in that the lower the wavenumber of the N–H stretch, the stronger the intermolecular hydrogen bonding. It was shown that for cyclo(D-Ala-L-Ala), the hydrogen bonding in polymorphic form 2 was stronger than in form 1.[4] This relationship can also be seen in the Raman spectrum of the two polymorphs of cyclo(L-Glu-L-Glu). For form 1, two weak vibrational bands can be observed in the Raman spectrum, which can be attributed to the N–H stretching vibrations at 3287 and 3218 cm^{-1}; both belonging to the *A* symmetry group. A weak third band occurs at 3064 cm^{-1} in both the *xz* and *yz* spectra, inferring *B* symmetry. For form 2, two weak Raman vibrational bands can be observed for the N–H stretch at 3193 and 3117 cm^{-1}, both belonging to the *A* symmetry group. Again, a third, very weak feature can be observed at 3067 cm^{-1}, which apparently has *B* symmetry. The N–H stretching vibrations of form 1 are ~100 cm^{-1} higher than that of form 2, and therefore it can be concluded that the hydrogen bonds involving the amide N–H group are weaker in form 1 than form 2. This assertion can be confirmed by comparing the hydrogen-bonding distances, from the X-ray structures of the two polymorphs, in Table S2(b) (Supporting Information). The hydrogen-bonding distance is smaller in form 2 than in form 1, resulting in stronger hydrogen bonding. Unfortunately, we were only able to collect the IR spectra for form 1, but it is quite apparent that here we can observe four bands due to the N–H stretching mode located at 3288, 3214, 3085, and 3063 cm^{-1}. It is not uncommon to observe numerous sub-bands attributed to the N–H stretch in other CDAPs,[4,8,13,15] and this has been previously reported to be due to either Fermi resonance and/or anharmonic coupling of the X–H stretch with lower wavenumber modes of the XH···YZ group.[13,32]

The O–H stretch of the carboxylic acid group appears clearly as a number of broad bands located between 2450 and 2760 cm^{-1} in the IR spectrum of form 1 of cyclo(L-Glu-L-Glu). An O–H stretch located in this region of the IR spectrum is typical when there is strong intermolecular hydrogen bonding involved. Indeed, it is well known that the intermolecular bonding of carboxylic acid groups can result in cyclic dimers that involve strong hydrogen bonds.[32] Again, it is apparent that many sub-maxima are observed for the O–H stretching vibrations. As stated earlier, this phenomenon can be attributed to anharmonic coupling with lower wavenumber vibrations associated with this mode.[13,32] The O–H stretching modes are of considerably lower intensity in the Raman spectra and can only be observed between 2550 and 2760 cm^{-1}. The O–H stretching band positions in the Raman spectra of forms 1 and 2 are very similar. This indicates that the strengths of the hydrogen bonds involving the carboxylic acid groups are very similar for both polymorphs. After *N*,*O*-deuteration, both Raman and IR spectra show a large downward shift in wavenumber. It is evident that we could not achieve 100% deuteration, as investigation of the IR spectra shows residual bands above 3000 cm^{-1}. Repeated deuteration steps did not improve this situation. In the Raman spectrum (form 1), a set of three bands at ~2350 cm^{-1} are assigned to the N–D stretching vibration of cyclo(L-Glu-L-Glu). Previous results from other CDAPs have shown that it is typical to find N–D stretching vibrations around this wavenumber.[4,8,13,15] Similar results are observed for polymorph form 2. The O–D stretch is assigned to two very weak, broad bands in the Raman spectra of forms 1 and 2, located at ~2200 and ~2100 cm^{-1}. In the IR spectrum, the N–D and O–D stretches are not only a lot more intense but also appear broader and more featureless than in the spectrum of the protonated species. The N–D stretch is assigned to a very broad feature at ~2250 cm^{-1}, whereas the two broad features located at 2200 and 2100 cm^{-1} are assigned to the O–D stretching vibration.

The C–H stretching region for cyclo(L-Glu-L-Glu) spans the region 2900–2990 cm^{-1}. These bands are more intense in the Raman than in the IR spectra. Band assignments can easily be

Journal of RAMAN SPECTROSCOPY

made by comparison with the DFT calculations, and additionally because they do not shift on *N*-deuteration.

The 1150–1700 cm^{-1} region

Normal vibrational modes found in this region include three peptide group vibrations (C═O stretch, C–N stretch, and N–H in-plane bending), carboxylic acid C═O stretch, C–O–H bending modes, C^{α}–H bends, and CH_2 scissoring, wagging, and twisting modes. Two strong bands are observed in the C═O stretching region in the IR spectrum of cyclo(L-Glu-L-Glu) form 1. These are located at 1708 and 1635 cm^{-1} and have been assigned to the C═O stretching vibration of the carboxylic acid group and the C═O stretching vibration of the amide group (*cis* amide I mode), respectively. It is surprising to note that no factor-group splitting is observed for these bands, as the IR spectrum for cyclo(L-Asp-L-Asp) shows four vibrational modes in this region, due to factor-group splitting.[15] The solid-state Raman spectrum of form 1 also only exhibits two bands in the carbonyl stretching region located at 1697 and 1653 cm^{-1}, both belonging to the *A* symmetry group. These are attributed to the C═O stretching vibration of the carboxylic acid group and the C═O stretching vibration of the amide group (*cis* amide I mode), respectively. Interestingly, it is worth noting that a weak band can be observed at 1612 cm^{-1} in the *yz* and *xz* single-crystal spectra. This mode obviously belongs to the *B* symmetry group. Although it is possible that this band is due to factor-group splitting from the amide carbonyl stretch, the splitting of the bands would be very large, of the order of 40 cm^{-1}. Previously, it has been suggested that a separation of ~40 cm^{-1} is too large for factor-group splitting in the amide I mode[13] of CDAPs, but perhaps these previous assertions should be revised. The solid-state Raman spectrum of cyclo(L-Glu-L-Glu) form 2 has a strong band at 1667 cm^{-1} and a weak shoulder at 1648 cm^{-1}. From the single-crystal spectra, it is evident that both of these vibrational modes belong to the *A* symmetry group, and they have been assigned to the factor group splitting modes of the C═O stretching vibration of the amide group. In the single-crystal spectrum *xy*, two new weak bands appear at 1708 and 1679 cm^{-1}, which are not present in the solid-state spectrum (C═O stretching vibration of the carboxylic acid group showing factor group splitting). Because these bands appear in the *xy* spectrum, they have been classified as belonging to the *A* symmetry group. In comparing form 1 with form 2, it should be noted that both the C═O stretch of the carboxylic acid and the amide group are ~10 cm^{-1} lower in form 1. These differences, again, show how the different hydrogen-bonding motifs found in the two polymorphs affect the vibrational spectra. Both of the C═O stretching vibrations (amide and carboxylic acid) shift down in wavenumber after deuteration. This, for example, can be observed in the Raman spectrum of form 1, where the C═O stretching vibration of the carboxylic acid group is shifted down by ~10 cm^{-1} and the amide I vibration is shifted down by ~20 cm^{-1}. The above result indicates a fairly small contribution from the N–H and/or O–H deformation to both these vibrational modes. In the aqueous solution Raman spectrum, it is possible to observe two bands at 1714 and 1668 cm^{-1}, which are assigned to the C═O stretching vibration of the carboxylic acid and the *cis* amide I modes, respectively. These bands are ~15 cm^{-1} higher than their counterparts in the solid-state Raman spectrum of form 1, but are similar to those in the solid-state Raman spectrum of form 2.

The C–N, *cis* amide II mode occurs at ~1493 cm^{-1} in the solid-state Raman spectrum for both polymorphs of cyclo(L-Glu-L-Glu) and at 1507 cm^{-1} in aqueous solution. No corresponding band is found in the IR spectrum. This band is, predominantly, an out of phase C^{α}–C–N stretch with a lower degree of contribution from the N–H in-plane bend than in the *trans* amide II mode.[13] Indeed, the *trans* amide II mode of linear L-Glu-L-Glu has been observed in the ~1570 cm^{-1} region of the Raman and IR spectra[16]; so in this respect there is quite a substantial difference between the *cis* and *trans* amide II modes. There is little difference between the location of the *cis* amide II mode in forms 1 and 2 in the Raman spectra of cyclo(L-Glu-L-Glu). Thus the different hydrogen-bonding motifs found in the two polymorphs have little effect on the location of this vibrational mode. Previously, we have noticed that (in the solid state) as the size (molecular weight) of the amino acid side chain (R group) increases, there is a decrease in the wavenumber of the C–N stretch (amide II). There also appears to be a link with respect to the conformation of the DKP ring, in that a boat conformation has a *cis* amide II mode lower in wavenumber than that with a planar/near planar DKP ring conformation. For example, the amide II vibrations in cyclo(Gly-Gly), cyclo(D-Ala-L-Ala), and cyclo(L-Ala-Gly) are observed at wavenumbers of 1517, 1523, and 1522 cm^{-1}, respectively,[4,13,15] whereas the amide II modes of cyclo(L-Glu-L-Glu), cyclo(L-Asp-L-Asp), and cyclo(L-Met-L-Met) are located at 1493, 1489, and 1493 cm^{-1}, respectively.[8,15] We hypothesise that this mass effect is possibly accompanied by an increase in the strain on the DKP ring in the solid state. The increase in ring strain must be brought about by crystal packing forces, because it is noticeable that in the aqueous-solution Raman spectrum of cyclo(L-Glu-L-Glu) the amide II mode shifts to higher wavenumber by ~15 cm^{-1}. Indeed, this apparent increase in wavenumber, on going from the solid to the aqueous state, is very small in the case of cyclo(Gly-Gly),[13] cyclo(D-Ala-L-Ala),[4] and cyclo(L-Ala-Gly),[15] in which there is less strain on the DKP ring from crystal packing forces. After deuteration, the *cis* amide II modes of both polymorphs of cyclo(L-Glu-L-Glu) display a downward shift of ~26 cm^{-1}, which shows that this band has a small N–H deformation contribution. Indeed, this shift is in good agreement with other CDAP *cis* amide II shifts after deuteration.[4,8,13,15] The *trans* amide II mode has a greater shift on *N*-deuteration; e.g. linear L-Met-L-Met displays a downward wavenumber shift of 66 cm^{-1}.[15] The foregoing observation indicates there is a significantly larger (N–H) contribution to the *trans* amide II band compared with the *cis* amide II band.

The majority of the bands occurring in between 1400 and 1470 cm^{-1} in both the Raman (forms 1 and 2) and IR (form 1) of cyclo(L-Glu-L-Glu) can be assigned to the CH_2 asymmetric or symmetric bending modes. These bands show negligible shift upon deuteration. The N–H bending vibration is difficult to locate in both the Raman and IR spectra. Previous results from other CDAPs have reported N–H bending vibrations between 1360 and 1460 cm^{-1}, showing how important the strength of hydrogen bonding is to this vibrational mode. In the Raman spectrum of cyclo(L-Glu-L-Glu), form 1, there is a broad, weak band located at 1373 cm^{-1}, which is tentatively assigned to the N–H bending vibration. This band apparently disappears after *N*-deuteration and is shifted down to around 1220 cm^{-1}. For form 2, there is a weak, broad vibrational band located at 1419 cm^{-1}, which shows a substantial deuterium shift. This is, again, tentatively assigned to the N–H bending vibration. If these assignments are correct, there is a ~45 cm^{-1} wavenumber difference between the N–H bending vibrations for the two polymorphs. This observation can be accounted for by the two different hydrogen-bonding motifs found in the crystalline lattices. It is difficult to assign an N–H

bending vibration in the IR spectrum, as quite a broad feature is observed spanning the 1400 cm^{-1} region. It is also very difficult to assess whether any of the shoulders on this peak are being shifted after deuteration. There are also bands that appear at 1351 cm^{-1} in the IR and 1344 cm^{-1} in form 1 (1351 cm^{-1} in form 2) in the Raman spectrum that show a significant shift after deuteration. This indicates that the vibrational mode has N–H character. Indeed, our DFT calculations predict PED contributions including N–C stretching, N–H in-plane bending, and C–C–H bending vibrations.

The bands found between 1320 and 1250 cm^{-1} in the Raman and IR spectra are attributed to vibrations which are quite mixed but generally show a major contribution due to $CC^{\alpha}H$ bending, wagging and/or CH_2 wagging modes. Some of these bands exhibit a small downward shift on deuteration, indicating contributions from N–H and/or C–O–H bending vibrations. There is little difference between the Raman spectra of form 1 and form 2 in this region of the vibrational spectrum, presumably indicating that the different crystal structures have no relevance to the band locations for these vibrational modes.

The vibrational mode in the IR spectrum located at 1263 cm^{-1} and in the Raman at ~1256 cm^{-1} in both forms 1 and 2 disappear after deuteration and show a downward shift in wavenumber. We tentatively assign these bands to the C–O–H bending vibration, although it is clear from the theoretical calculations that these modes are mixed with $CC^{\alpha}H$ bending and CH_2 wagging motions. New bands appear in the IR spectrum upon deuteration at ~1040 cm^{-1}, and in the Raman spectra a new feature appears at ~1060 cm^{-1}. These features are assigned to the C–O–D bending vibration. The assignments are made more realistic by comparison with the vibrational spectrum of a similar molecule such as cyclo(L-Asp-L-Asp).[15] Here, an analogy can be made, as vibrational modes in the IR spectrum at 1245 and 1242 cm^{-1} in the Raman spectrum, which have been assigned to the C–O–H bending vibration, show a deuterium shift too ~1050 cm^{-1}.

The weak features found between 1200 and 1220 cm^{-1} in both solid-state Raman spectra of form 1 and 2 of cyclo(L-Glu-L-Glu) are assigned to the CH_2 twisting vibrations. These bands, although mixed, do not show any significant deuterium shift, thus indicating that there is no mixing with N–H or O–H bending vibrations.

The 825–1200 cm^{-1} region

The bands that occur in this region are due to $N–C^{\alpha}$ and C–C stretching as well as to C–O stretching and CH_2 rocking and twisting vibrations. The IR and Raman spectra have one band located at ~1195 cm^{-1}. This band shows negligible shift upon deuteration, and the calculated PEDs suggest that this mode is primarily associated with CH_2 twisting vibration. Previously, the bands in the 1100–1200 cm^{-1} region have been associated with $N–C^{\alpha}$ stretching vibrations,[4,8,13,15] but our calculations suggest that the PEDs do not contain any significant N–C stretching character. The C–O stretching vibration appears in the PEDs of two vibrational modes found in both Raman spectra of the two polymorphs of cyclo(L-Glu-L-Glu). Again, there is very little difference between the locations of these vibrations for form 1 and 2, in which both bands are observed at ~1144 and 1122 cm^{-1}. This highlights the fact that the C–O stretching vibration shows little sensitivity to the different crystal lattices. The C–O stretching vibrations are shifted on deuteration, showing that these modes also include C–O–H bending character as inferred in the calculations highlighted in Table 2. It is not very clear where these bands are shifted to after deuteration, but it is thought that they may have emerged as one of a series of bands at ~1060 cm^{-1}. The C–O stretching vibration is also observed in the IR spectrum, which shows a similar deuterium shift as described above. It is worth noting that the assignments can be confirmed due to the great similarity of the vibrational spectra in this region with that of cyclo(L-Asp-L-Asp).[15]

The assignment of bands between 1090 and 840 cm^{-1} is quite complicated because they are due to modes which generally involve a very high degree of mixing. The DFT calculations show that the C–C stretching vibrations make a contribution to all modes found in this region. The calculations also predict that some of the bands found between 825 and 1060 cm^{-1} can be assigned to C–C–H and CH_2 rocking modes. This is supported by analogy with assignments for other CDAPs.[4,8,13,15] The most intense Raman band in the spectrum of cyclo(L-Glu-L-Glu) form 1 is located at 925 cm^{-1}. A very strong band at the same location is observed in the spectrum of form 2. It appears that this band is due, predominantly, to C–C stretching, but it is also possible that ring bending also contributes. After deuteration (Raman spectrum, form 1), there is a downward shift (~20 cm^{-1}) and a considerable loss in intensity. The small downward shift is indicative of this vibrational mode being coupled to the N–H or O–H moieties.

The 500–820 cm^{-1} region

In this region, there are two peptide group vibrations: N–H out-of-plane bending and C=O bending modes. Other vibrations in this region include ring bending, ring deformations, ring stretching bands, and O–C=O bending modes. We can tentatively assign two broad medium-intensity bands located at 752 and 734 (sh) cm^{-1} in the IR spectrum of cyclo(L-Glu-L-Glu) form 1 to the N–H out-of-plane bending (opb) vibration. These assignments have been made with respect to the spectra of the *N*,*O*-deuterated species, where a considerable downward shift can be observed with two new bands appearing at 578 and 550 cm^{-1}. Previous work has shown that the NH opb of, for example, cyclo(Gly-Gly), (L-Ala-Gly), and (L-Met-L-Met) gives rise to a broad feature centred around ~820 cm^{-1} in the IR,[8,13,15] but in the case of cyclo(L-Ser-L-Ser)[15] and cyclo(L-Asp-L-Asp)[15] broad features corresponding to the N–H opb have been found in the 700 cm^{-1} region. We have previously suggested that this phenomenon could be due to the nature of the hydrogen bonding involved in the crystal lattice, and it should be noted that both cyclo(L-Ser-L-Ser) and (L-Asp-L-Asp) have substituents on the C^{α} as well as the amide groups that can partake in hydrogen-bonding, whereas cyclo(Gly-Gly), (L-Ala-Gly), and (L-Met-L-Met) only have the N–H and C=O of the amide group to partake in intermolecular hydrogen bonding.[8,13,15] Unfortunately, we could not compare the N–H opb vibration in the IR spectra of the two polymorphs, because there was insufficient material available. In the Raman spectra of cyclo(L-Glu-L-Glu), for both forms 1 and 2 it is very difficult to assign the N–H opb due to the very low intensity of this mode. Despite this, possible candidates may be the weak/broad band located at 737 cm^{-1} in the Raman spectrum of form 1, and the weak/broad band observed at 762 cm^{-1} in form 2. Both these bands, in the two polymorphs, are tentatively assigned to the N–H opb because of considerable shifts after *N*-deuteration.

The bands located in the 500–700 cm^{-1} range are attributed to vibrations that are quite mixed but generally contain significant PEDs relating to the carbonyl groups. In the Raman spectrum of cyclo(L-Glu-L-Glu), form 1, there are a series of bands between 600

and 700 cm^{-1}. The bands close to ~680 cm^{-1} are quite weak and appear to be predominantly C=O opb modes of the amide group, whereas the weak bands close to 660 cm^{-1} exhibit a high degree of character from C=O twisting of the carboxylic acid group. A medium-sized doublet is located at 640 and 633 cm^{-1}, which is assigned to vibrations involving both C=O ipb of the amide group and O–C=O bend of the carboxylic acid group. This doublet is shifted down by ~25 cm^{-1} after deuteration, thus indicating that this mode involves motion of either N–H or O–H moieties. In the Raman spectrum of form 2, there are slight differences from that of form 1, where a broader, more featureless band is observed at ~680 cm^{-1} and a band of strong intensity is located at ~645 cm^{-1}, but on the whole the assignments are the same as for form 1. In the IR spectrum of cyclo(L-Glu-L-Glu) form 1, a medium intensity band is observed at 658 cm^{-1} which, as our DFT calculations suggest, should be (predominately) a C=O twisting vibration of the carboxylic acid group, but we would also expect to see a medium intensity band in this region of the IR spectrum for the C=O opb of the amide group. The other IR bands in this region are very, very weak.

Two weak broad bands are observed at 587 and 570 cm^{-1} in the Raman spectrum of form 1, which, from our calculations, are assigned to a vibration dominated by O–C=O wagging. Only one broad band can be observed at 588 cm^{-1} in the Raman spectrum of form 2.

Bands below 500 cm^{-1}

In general, the assignments of bands in this region of the spectrum are not straightforward, but tentative assignments have been made possible by comparison with the calculated spectra.

In the 400–499 cm^{-1} region of the Raman spectrum, there are four bands of similar location in both forms 1 and 2. The first is of medium intensity in form 1 and strong in form 2 and is located at 495 cm^{-1}. Our calculations predict that this vibration is predominantly due to ring bending but may also contain the amide C=O in-plane bend character. Two weaker bands appear at 483 and 452 cm^{-1}, which tentatively have been assigned to a O–C=O rocking vibration due to its high PED contribution. The Raman band at 406 cm^{-1} is attributed to a mixed vibration that involves CCH and C=O bending vibrations.

The bands that occur in the 200–400 cm^{-1} region of the Raman spectrum are assigned to vibrations that are of very mixed character, and are predominantly due to ring, C=O, C–C, C–C–O bending and C–C–H rocking as well as torsional motions.

The bands located between 50 and 200 cm^{-1} again are also very mixed, and are mainly due to ring bending vibrations, torsional vibrations of the aliphatic chain attached to the C^{α} atom, and lattice vibrations. The bands in this region show no significant shift on *N*-deuteration, indicative of very little N–H contribution to these modes.

Conclusions

Cyclo(L-Glu-L-Glu) has been found to crystallise into at least two different polymorphic forms. X-ray crystallographic studies have shown that both crystalline polymorphs are monoclinic, with two molecules per unit cell, but form 1 has a space group $P2_1$ and form 2 has a space group C_2. The crystal structures are different by virtue of different hydrogen-bonding schemes. In form 1 there are H-bonded layers involving four hydrogen bonds, whereas in form 2 only one unique H-bond is involved plus the 2-fold generated ones. The calculated structure for cyclo(L-Glu-L-Glu), based on full geometry optimisation with C_2 symmetry, predicts a boat conformation for the DKP ring with both L-Glu side chains being folded above the ring. The calculated geometry of the boat conformation shows good agreement with that of the X-ray structure. There is a good correlation between the calculated and X-ray structures, with the exception of the bond lengths and bond angles involving the hydrogen bonded N–H group. Indeed, this problem also means that there are differences between the calculated and experimental vibrational spectra with respect to modes containing a high N–H contribution to the PED.

Differences between the Raman spectra of the polymorphic forms of cyclo(L-Glu-L-Glu) are observed particularly with respect to the N–H stretching and *cis* amide I vibrations. The N–H stretching vibrations of form 1 are ~100 cm^{-1} higher than that of form 2, and therefore it can be concluded that the hydrogen bonds involving the amide N–H group are weaker in form 1 than form 2. This is confirmed by the hydrogen-bond lengths in the X-ray structure. The two common hydrogen bonding motifs found in CDAPs are known as 'chains' and 'layers'. Indeed, in the absence of an X-ray structure, Raman spectroscopy may provide insight into the strength of hydrogen bonding and therefore the hydrogen-bonding pattern. The *cis* amide I vibration of the two polymorphs are separated by 10 cm^{-1}, indicating that this vibration is less sensitive to hydrogen–bonding strength.

The N–H opb can be observed in the IR spectrum of form 1 between 730 and 750 cm^{-1}. This result is similar to that for cyclo(L-Ser-L-Ser) and cyclo(L-Asp-L-Asp) but quite different from a number of other CDAPs[15] [cyclo(Gly-Gly),[13] (L-Ala-L-Ala),[15] (L-Met-L-Met)],[8] which have an N–H opb at ~820 cm^{-1}. This lower N–H opb has been suggested to be due to the nature of the hydrogen bonding involved in the crystal lattice; cyclo(L-Glu-L-Glu), cyclo(L-Ser-L-Ser), and cyclo(L-Asp-L-Asp) have two substituents: one on the C^{α} and one on the amide group, which can partake in hydrogen bonding.

Acknowledgements

R. Withnall and B. Z. Chowdhry would like to acknowledge the EPSRC (Instrument Grant, Ref. GR/L85176), and Horiba Jobin Yvon for jointly funding the purchase of the Labram Raman spectrometer. We thank the EPSRC X-ray Data Collection Service, Southampton, for help with data collection.

Supporting information

Supporting information may be found in the online version of this article.

References

[1] R. L. Bowman, M. Kellerman, W. Curtis Johnson Jr *Biopolymers* **1983**, *22*, 1045.
[2] E. J. Sletten, *Am. Chem. Soc.* **1970**, *92*, 172.
[3] J. Sletten, *Acta Chem. Scand. A* **1980**, *34*, 593.
[4] T. C. Cheam, S. Krimm, *Spectrochim. Acta* **1988**, *44A*, 185.
[5] R. Degeilh, R. E. Marsh, *Acta Crystallogr.* **1959**, *12*, 1007.
[6] G. G. Fava, M. F. Belicchi, *Acta Crystallogr. B* **1981**, *37*, 625.
[7] G. Vallé, V. Guantieri, T. A. Tamburro, *J. Mol. Struct.* **1990**, *220*, 19.
[8] A. P. Mendham, B. S. Potter, R. A. Palmer, T. J. Dines, J. C. Mitchell, R. Withnall, B. Z. Chowdhry, *J. Raman Spectrosc.* **2009**, in press. DOI:10.1002/jrs2426.

[9] G. Tayhas, R. Palmore, T. M. Luo, M. T. Mc Bride-Wieser, E. A. Picciotto, M. Reynoso-Paz, *Chem. Mat.* **1999**, *11*, 3315.
[10] D. B. Davies, Md. A. Khalad, *J. Chem. Soc. Perkins Trans.* **1975**, *2*, 1238.
[11] K. D. Kopple, V. Narutis, *Int. J. Pept. Protein Res.* **1981**, *18*, 33.
[12] F. L. Bettens, R. P. A. Bettens, R. D. Brown, P. D. Godfrey, *J. Am. Chem. Soc.* **2000**, *122*, 5856.
[13] T. C. Cheam, S. Krimm, *Spectrochim. Acta* **1984**, *40A*, 481.
[14] Y. Zhu, M. Tang, X. Shi, Y. Zhao, *Int. J. Quantum Chem.* **2007**, *107*, 745.
[15] (a) A. P. Mendham, T. J. Dines, M. J. Snowden, B. Z. Chowdhry, R. Withnall, *J. Raman Spectrosc.* **2009**, In Press. DOI 10.1002/jrs.2293; (b) A. P. Mendham, T. J. Dines, M. J. Snowden, R. Withnall, B. Z. Chowdhry, *J. Raman Spectrosc.* **2009**, In Press. DOI 10.1002/jrs.2306; (c) A. P. Mendham, T. J. Dines, R. Withnall, J. C. Mitchell, B. Z. Chowdhry, *J. Raman Spectrosc.* **2009**, In Press. DOI 10.1002/jrs2307.
[16] J. T. Lopez Navarette, V. Hernandez, F. J. Ramirez, *J. Mol. Struct.* **1995**, *348*, 249.
[17] Enraf-Nonius, CAD-4 Software, Enraf-Nonius, Delft, Holland, **1988**.
[18] G. M. Sheldrick, *SHELX86: Program for The Solution of Crystal Structures*, University of Göttingen: Germany, **1986**.
[19] G. M. Sheldrick, *SHELX97: Program for The Refinement of Crystal Structures*, University of Göttingen: Germany, **1993**.
[20] L. J. Farrugia, *J. Appl. Crystallogr.* **1988**, *32*, 837.
[21] L. A. Spek, *Acta Crystallogr.* **1990**, *A46*, 194.
[22] C. L. Barnes, *J. Appl. Crystallogr.* **1997**, *30*, 568.
[23] POV-Ray™ rendering engine for Windows. Version 3.1 g.watcom.win32 [Pentium II Optimized], **1994**.
[24] H. D. Flack, *Acta Crystallogr.* **1983**, *A39*, 876.
[25] M. A. Robb, J. R. Cheeseman, V. G. Zakrzewski, J. A. Montgomery Jr, R. E. Stratmann, J. C. Burant, S. Dapprich, J. M. Millam, A. D. Daniels, K. N. Kudin, M. C. Strain, O. Farkas, J. Tomasi, V. Barone, M. Cossi, R. Cammi, B. Mennucci, C. Pomelli, C. Adamo, S. Clifford, J. Ochterski, G. A. Petersson, P. Y. Ayala, Q. Cui, K. Morokuma, D. K. Malick, A. D. Rabuck, K. Raghavachari, J. B. Foresman, J. Cioslowski, J. V. Ortiz, B. B. Stefanov, G. Liu, A. Liashenko, P. Piskorz, I. Komaromi, R. Gomperts, R. L. Martin, D. J. Fox, T. Keith, M. A. Al-Laham, C. Y. Peng, A. Nanayakkara, C. Gonzalez, M. Challacombe, P. M. W. Gill, B. Johnson, W. Chen, M. W. Wong, J. L. Andres, C. Gonzalez, M. Head-Gordon, E. S. Replogle, J. A. Pople, *Gaussian 98, Revision A.6*, Gaussian, Inc.: Pittsburgh, **1998**.
[26] A. D. Becke, *J. Chem. Phys.* **1993**, *98*, 5648.
[27] C. Lee, W. Yang, R. G. Parr, *Phys. Rev. B* **1988**, *37*, 785.
[28] T. J. Dunning Jr, *J. Chem. Phys.* **1989**, *90*, 1007.
[29] J. A. Schachtschneider, *Vibrational Analysis of Polyatomic Molecules, Parts V and VI*, Technical Report No. 57, 231, Shell Development Co.: Houston, **1964,1965**.
[30] P. Pulay, G. Fogarasi, F. Pang, J. E. Boggs, A. Vargha, *J. Am. Chem. Soc.* **1983**, *105*, 7037.
[31] K. I. Varughese, C. T. Lu, G. Kartha, *Int. J. Pept. Protein Res* **1981**, *18*, 88.
[32] L. J. Bellamy, *The Infrared Spectra of Complex Molecules*, vol. 2, Chapman and Hall: London, **1980**.